THE JOURNAL OF BIOLOGICAL CHEMISTRY
Vol. 278, No. 9, Issue of February 28, pp. 7285–7293, 2003
Printed in U.S.A.

Role of an Intrasubunit Disulfide in the Association State of the Cytosolic Homo-oligomer Methionine Adenosyltransferase*

Received for publication, October 4, 2002, and in revised form, December 12, 2002
Published, JBC Papers in Press, December 20, 2002, DOI 10.1074/jbc.M210177200

Gabino F. Sánchez-Pérez‡, María Gasset§, Juan J. Calvete¶, and María A. Pajares‡‖

From the ‡Instituto de Investigaciones Biomédicas "Alberto Sols," Consejo Superior de Investigaciones Científicas (CSIC)-Universidad Autónoma de Madrid, Arturo Duperier 4, 28029 Madrid, Spain, the §Instituto de Química-Física "Rocasolano," CSIC, Serrano 119, 28006 Madrid, Spain, and the ¶Instituto de Biomedicina de Valencia, CSIC, Jaime Roig 11, 46006 Valencia, Spain

Recombinant rat liver methionine adenosyltransferase has been refolded into fully active tetramers (MAT I) and dimers (MAT III), using as a source chaotrope-solubilized aggregates resulting from specific washes of inclusion bodies. The conditions of refolding, dialysis in the presence of 10 mM dithiothreitol or 10 mM GSH with 1 mM GSSG, allowed the production of both isoforms, the nature of the redox agent determining the capacity of the final product (MAT I/III) to interconvert. Refolding in the presence of 10 mM dithiothreitol yielded mainly MAT III in a concentration-dependent equilibrium with the homotetramer MAT I. However, refolding in the presence of the redox pair GSH/GSSG resulted in a stable MAT I and III mixture. Blockage of dimer-tetramer interconversion has been found related to the production of a single intramolecular disulfide in methionine adenosyltransferase during the GSH/GSSG folding process. The residues involved in this disulfide have been identified by mass spectrometry and using a set of single cysteine mutants as cysteines 35 and 61. In addition, a kinetic intermediate in the MAT I dissociation to MAT III has been detected. The physiological importance of these results is discussed in light of the structural and regulatory data available.

Cysteines are one of the least abundant but highly reactive amino acids present in polypeptide chains. Their appearance is, in many cases, related to a key role of the sulfhydryl group on the structural and functional features of the protein. These side chains have the capacity to actively participate in catalysis, can be posttranslationally modified, or can lead to the apparition of redox sensitive sites that could have effects either on modulation of catalysis or because of the generation of conformational restrictions (1–3). Posttranslational modifications, such as prenylation and acylation, take place in the sulfhydryl group of cysteine residues located at or near the C terminus of the protein, leading to translocation from the cytosol to membranes (4, 5). Nitrosylation occurs in residues related to activity control, either activating (ryanodine receptor) or inactivating key proteins (MAT)[1] (6). Zinc chelation determines the acquisition of polypeptide geometries compatible with the recognition of nucleic acids (zinc fingers) (7). Moreover, the presence of cysteine sulfhydryl groups may also play an essential role in folding and association, because of disulfide bond formation (8, 9). To form this covalent bond, the residues must come to a distance such that the Cα atoms of the cysteines are within 3.8–4.5 Å of each other (9). These disulfides can be established within the same subunit, linking different areas of the polypeptide chain that may be quite distant in the sequence, or between subunits, binding each monomer on the right position to the others (10, 11).

The production and stability of disulfides have been related to the existence of an oxidative environment. Thus, the number of extracellular or secreted proteins that contain disulfide bridges in their structure is large, because of their passage through a highly oxidative environment, such as that of the endoplasmic reticulum, where the presence of thiol/disulfide oxidoreductases favors their production (12). However, *in vitro* experiments have demonstrated that it is possible to obtain disulfide bonds even under strong reducing conditions, provided the local concentration of sulfhydryls is high enough (13). Therefore, the presence of disulfides in cytosolic proteins is possible, and in fact, there have been some reports describing their existence (14, 15). The role for these covalent bonds is not clear and may be related to the control of protein activity.

One of the few cases where the presence of a cytosolic disulfide has been described is the liver-specific methionine adenosyltransferase (MAT), a homo-oligomeric protein that is isolated as stable tetramers (MAT I) and dimers (MAT III), differing in the affinity for methionine (16). MAT I is 10-fold more active than MAT III under physiological concentrations of the amino acid (60 μM) (17), and hence the ratio of isoforms determine the activity level displayed in the cell. This is of special relevance if we take into account that the product of MAT reaction is *S*-adenosylmethionine, the main methyl donor for the transmethylation reactions (18). This enzyme presents 10 cysteine residues/subunit (19, 20), and under several *in vitro* and *in vivo* conditions it has been possible to demonstrate their role on the activity and oligomeric state: (*a*) inactivation and dissociation of MAT I is produced by *N*-ethylmaleimide (NEM) modification of two −SH groups (21, 22); (*b*) site-directed mutagenesis of Cys^{69} renders the enzyme mainly as dimers (23); (*c*) all of the mutants on the cysteines comprised between

* This work was supported by Fondo de Investigación Sanitaria Grant 01/1077 (to M. A. P.), Dirección General de Investigación Científica y Técnica Grant PM 97/0064 (to M. A. P.), Ministerio de Ciencia y Tecnologia Grant BMC 2002-00243 (to M. A. P.), and Neuropharma Grants SA-CSIC (to M. G. and M. A. P.) and BMC2001-3337 (to J. J. C.). The costs of publication of this article were defrayed in part by the payment of page charges. This article must therefore be hereby marked "*advertisement*" in accordance with 18 U.S.C. Section 1734 solely to indicate this fact.

‖ To whom correspondence should be addressed. Tel.: 34-91-5854414; Fax: 34-91-5854401; E-mail: mapajares@iib.uam.es.

[1] The abbreviations used are: MAT, ATP:L-methionine adenosyltransferase; DTT, dithiothreitol; NEM, *N*-ethylmaleimide; ANS, 8-anilinonaptht halene-1-sulfonic acid; EP, ethylpyridylated; c-MAT, *E. coli* methionine adenosyltransferase; MALDI-TOF, matrix-assisted laser desorption ionization time-of-flight; CM, carboxyamidomethylated.

residues 35 and 105 have some effect on the MAT I/MAT III ratio (23); (*d*) the enzyme activity is inhibited by GSSG (2) and nitrosylation of Cys^{121} (24, 25); (*e*) inhibition of the glutathione synthesis leading to a 30% reduction in the GSH levels, and hence to the alteration of the GSH/GSSG ratio, correlates with a decrease in MAT activity (26); and (*f*) low MAT activity and mainly dimers are detectable under the oxidative conditions of alcohol liver cirrhosis (27). Moreover, a disulfide bond between Cys^{35} and Cys^{61} that are located in the β-sheet of contact between dimers, according to the crystal structure, has been identified (15, 28). This disulfide was not detected when the protein was overexpressed in *Escherichia coli*, where MAT I/III appears in a concentration-dependent equilibrium (29), thus suggesting a role for it on the association. The aim of this paper is to demonstrate the key role of the disulfide on MAT assembly; this, to the best of our knowledge, is the first description of such a role for this type of covalent bond in a cytosolic oligomer.

EXPERIMENTAL PROCEDURES

Materials

Methionine, ATP, phenylmethanesulfonyl fluoride, pepstatin A, aprotinin, leupeptin, antipain, DTT, ampicillin, GSH, GSSG, cyanogen bromide, 4-vinylpyridine, iodoacetamide, and the molecular mass standards for gel filtration chromatography were products from Sigma. NEM and trypsin sequencing grade were purchased from Serva (Heidelberg, Germany) and Roche Diagnostics (Barcelona, Spain), respectively. [2-^{3}H]ATP (20 Ci/mmol) and [1,4 ^{14}C]NEM (2–10 mCi/mmol) were supplied by Amersham Biosciences and ARC Inc. (St. Louis, MO), respectively. Isopropyl-β-D-galactopyranoside was a product of Ambion (Austin, TX). Phenyl Sepharose CL-4B and Superose 12 HR 10/30 were purchased from Amersham Biosciences. Optiphase HiSafe 3 scintillation fluid was obtained from E & G Wallac (Milton Keynes, UK). Cation exchanger AG-50W-X4, goat anti-rabbit IgG-horseradish peroxidase, Bio-Rad protein assay kit I, and the electrophoresis reagents were from Bio-Rad. YM-30 ultrafiltration membranes and glass microfiber filters GF/B were purchased from Amicon Corp. (Beverly, MA) and Whatman Ltd. (Maidstone, UK), respectively. Chemiluminescence Renaissance reagents and BCA were obtained from PerkinElmer Life Sciences and Pierce, respectively. Urea, Me_2SO, and Triton X-100 were purchased from Merck. The rest of the buffers and reagents were of the best quality commercially available.

Methods

Rat Liver MAT Expression, Refolding, and Purification—Competent *E. coli* BL21(DE3) cells were transformed with the plasmid pSSRL-T7N, which contains the sequence of wild type MAT, or the mutants for the cysteine residues of the protein (23). The cells were grown on LB medium plus ampicillin and expression induced by the addition of isopropyl-β-D-galactopyranoside (30). The inclusion bodies were isolated after disruption of the cells by sonication and purified as described by López-Vara *et al.* (31). Refolding was carried out using either 10 mM DTT or a redox buffer composed by GSH/GSSG (10:1) at 10 mM GSH. Purification of the DTT-refolded proteins was carried out as previously described but using a Q-Sepharose column (31), whereas GSH/GSSG-refolded MATs needed an additional purification step on phenyl Sepharose. The purity of the samples was tested by SDS-PAGE, and the final protein samples were characterized by fluorescence and circular dichroism spectroscopies.

MAT Association/Dissociation Studies by Analytical Gel Filtration and Phenyl Sepharose Chromatographies—Purified samples were concentrated by ultrafiltration through YM-30 membranes to obtain the desired range of protein concentrations. Samples of 100 μl were injected on a Superose 12 HR 10/30 gel filtration column connected to an Advanced Protein Purification System (Waters) and eluted using 50 mM Tris/HCl, pH 8, 10 mM $MgSO_4$ (buffer A) containing 150 mM KCl at a flow rate of 0.3 ml/min. A_{280} was recorded, and 210-μl fractions were collected for their use in dot blot and MAT activity measurements. The peak and shoulder corresponding to GSH/GSSG-refolded MAT III and I, respectively, were concentrated and reloaded on the same column, and their elution volumes were determined as above.

In parallel, 2-ml samples of the same protein concentrations were loaded on 3-ml phenyl Sepharose columns equilibrated in buffer A, washed with 20 ml of the equilibration buffer, and eluted with 10 ml of buffer A containing 50% (v/v) Me_2SO. Only the first 5-ml fractions of sample loading (MAT I) and Me_2SO elution (MAT III) were used for dot blot, MAT activity, and protein concentration measurements. Moreover, to follow dissociation MAT I fractions were collected, diluted 5-fold with buffer A, and incubated for 30 min prior to reloading on new phenyl Sepharose columns. Again fractions corresponding to MAT I and MAT III were collected and used for dot blot, MAT activity, and protein concentration measurements.

Dissociation Followed by ANS Binding—A 50 mM stock solution of ANS in methanol was prepared, and its concentration was determined using $\epsilon_{370} = 6800\ M^{-1}\ cm^{-1}$ (32). ANS was added to a 20-μl MAT I sample (1–4 mg/ml) to render a final concentration, upon dilution (1:50), of 40 μM, and to pre-equilibrated MAT III solutions (1 ml) of 20–80 μg/ml. Controls for each case were prepared accordingly, and the reaction was carried out for 1 h at room temperature in the dark. The final methanol concentration in the samples was 0.08% (v/v). Fluorescence emission at 470 nm was recorded for 8 min upon excitation at 380 nm in a photon counting SLM-8000 spectrofluorometer. MAT I kinetics were recorded immediately after dilution with a dead time 5 s. The data were corrected for base line and instrumental factors and adjusted to one- or two-phase exponential decays using the program GraphPad Prism (GraphPad Software Inc., San Diego, CA) and the following equations.

$$Y = Ae^{-kt} + Y_\infty \quad \text{(Eq. 1)}$$

$$Y = Ae^{-Xt} + Ae^{-Zt} + Y_\infty \quad \text{(Eq. 2)}$$

where Y is the fluorescence intensity at 470 nm; A is the amplitude of the signal; t is the time; k, X, and Z, the rate constants; and Y_∞ is the fluorescence intensity at an infinite time.

Large-zone Gel Filtration Chromatography—The dissociation constants were determined using a Biogel A gel filtration column (0.7 × 9 cm) equilibrated in buffer A containing 150 mM KCl. The column was run at 25 °C at a flow rate of 0.23 ml/min, and the accuracy of the flow was controlled by weighting fractions collected before and after each individual run (33). Purified proteins, wild type and mutants, were concentrated by ultrafiltration, as described above, to obtain the desired range of protein concentrations (0.05–5 mg/ml), and 3.5 ml of large zones were collected. Loading was performed at least 1 h after sample preparation to ensure equilibrium. Elution was followed by A_{280} and dot blot analysis of the 75-μl fractions collected. The data obtained by both methods were used to determine the centroid volume for each zone using GraphPad Prism. The centroid volumes were then used to calculate the weight-average partition coefficient (σ_w) and the corresponding dimer fraction (f_D) according to the following equations.

$$\sigma_w = (V_c - V_o)/V_i \quad \text{(Eq. 3)}$$

$$f_D = (\sigma_W - \sigma_T)/(\sigma_D - \sigma_T) \quad \text{(Eq. 4)}$$

where V_c is the centroid volume for the large zone; V_o is the void volume; V_i is the included volume of the column; σ_T is the partition coefficient for the tetramer; and σ_D is the partition coefficient of the dimer determined experimentally.

A plot of f_D *versus* log of the dimer concentration allows calculation of the equilibrium constant. f_D values were also used to determine the free energy of the process using equations analogous to those described by Park and Bedouelle (34) for a dimer-monomer equilibrium.

$$K f_D + 4c f_D^2 - K = 0 \quad \text{(Eq. 5)}$$

$$\Delta G = \Delta G(H_2O) - mx = -RT \ln(K) \quad \text{(Eq. 6)}$$

The total free energy of the process, from MAT I to the unfolded protein, can be calculated using the following expression.

$$\Delta G_{tot} = \Delta G_1 + 2\Delta G_2 \quad \text{(Eq. 7)}$$

where f_D is the fraction of protein as dimer; c is the protein concentration; R is the gas constant; T is the absolute temperature; ΔG is the free energy of the process; ΔG_1 is the free energy of the tetramer-dimer conversion; ΔG_2 is the free energy calculated for the dimer-monomer unfolding; m in this particular case is the slope of the dependence of the thermodynamical parameter upon protein concentration; ΔG_{tot} is the free energy of the total process, tetramer to monomer unfolding; and K is the equilibrium constant.

Dot Blot—The samples of the column fractions (maximum volume, 30 μl) were spotted on nitrocellulose membranes. After denaturation using 6 M guanidinium chloride (50 μl), the membrane was washed twice with TTBS (20 mM Tris/HCl, pH 7.5, 500 mM NaCl, 0.05% (v/v) Tween 20), before the blocking step using low fat dry milk (3% w/v).

The membrane was washed again with TTBS and incubated with a 1:20000 (v/v) solution of an anti-MAT polyclonal antibody prepared in our laboratory using DTT-refolded MAT. Under these conditions the only band detected corresponds to MAT in SDS-PAGE gels. The membranes were revealed using Renaissance, the exposed films were subjected to densitometric scanning, and the data were used for the corresponding calculations.

Determination of the Free Sulfhydryl Content and Location of the Disulfide Bond—The number of free −SH groups for wild type and mutant MATs was determined as described previously using NEM labeling (15, 22). In addition, for quantitation of free cysteine residues and disulfide bonds in wild type and mutant MAT proteins, samples of the purified proteins were dialyzed against ammonium acetate extensively and lyophilized, and the content of reduced and oxidized cysteine residues was determined by mass spectrometry. To this end, ~1 mg/ml of protein in 150 mM Tris/HCl, pH 8.6, 1 mM EDTA, 6 M guanidinium chloride was heated for 5 min at 80 °C, cooled down to room temperature, incubated either with 10 mM iodoacetamide for 1 h at room temperature or with 1% 2-mercaptoethanol for 2 min at 100 °C, followed by the addition of a 5-fold molar excess of 4-vinylpyridine or iodoacetamide over reducing agent, and incubated for 1 h at room temperature. The samples were dialyzed against deionized MilliQ water and lyophilized. Aliquots of these samples were subjected to matrix-assisted laser desorption ionization time-of-flight (MALDI-TOF) mass spectrometry using a PE Biosciences Voyager DE-Pro instrument and sinapinic acid (saturated in 0.1% trifluoroacetic acid in 50% acetonitrile) as matrix.

To locate free cysteines and disulfide bonds within the primary structure of MAT (Swiss-Prot S06114), native and ethylpyridylated proteins (10 mg/ml in 70% formic acid) were degraded with cyanogen bromide (100 mg/ml) overnight in the dark under a nitrogen atmosphere. In addition, native and carboxyamidomethylated proteins (1 mg/ml in 100 mM ammonium bicarbonate, pH 8.3, 10 mM iodoacetamide) were degraded with sequencing grade trypsin at an enzyme/substrate ratio of 1:50 (w/w) overnight at 37 °C. Mass fingerprinting of the digests was done by MALDI-TOF mass spectrometry using α-cyanocinnamic acid (saturated in 0.1% trifluoroacetic acid in 50% acetonitrile) as matrix.

N-terminal Sequencing—N-terminal sequence analyses of the purified wild type and mutant MAT proteins were done using an Applied Biosystems 473A sequencer following the manufacturer's instructions. The results indicated that 70% of the protein had a complete N-terminal sequence (MNGPVDGL), whereas the rest had lost the initial methionine. These data were taken into account in the MALDI-TOF mass spectrometry calculations.

Sedimentation Velocity Experiments—The samples (0.1–5 mg/ml) were loaded on the An50Ti rotor of a Beckman Optima XL-A analytical ultracentrifuge (Beckman Instruments Inc.) equipped with absorbance optics, and the experiments were performed at 50,000 rpm and 18 °C. Absorbance scans (step size, 0.005 cm) were taken at 280 nm. The sedimentation velocity data were analyzed with the program Svedberg (35), and the sedimentation velocity coefficients were corrected for solvent composition and temperature to obtain $s_{20,W}$ (36).

Determination of the Protein Concentration—Protein concentration of the samples after ultrafiltration was measured using the Bio-Rad kit I and using bovine serum albumin as a standard. However, protein concentration on the fractions collected from analytical phenyl Sepharose columns was determined after trichloroacetic acid precipitation using the BCA system, because of the presence of Me_2SO.

MAT Activity Measurements—MAT activity was measured as described by Gil *et al.* (37) using 160-μl samples of the column fractions. Kinetics for methionine and ATP were performed in the concentration range comprised from 1 μM to 10 mM for one of the substrates while keeping the other constant at 5 mM (2). Oxidation constants and GSSG inhibition were measured as previously described (2, 38).

RESULTS

Association/Dissociation Processes in Liver-specific MAT—Rat liver MAT has been shown to appear in a concentration-dependent equilibrium upon its overexpression in *E. coli* cytosol. However, there are no indications that such equilibrium takes place in the rat liver-purified enzyme forms. In an attempt to clarify the difference among these proteins and get insight into the structure-function facts that regulate MAT oligomerization, we have used two refolding systems described previously in our laboratory. The use of DTT rendered only

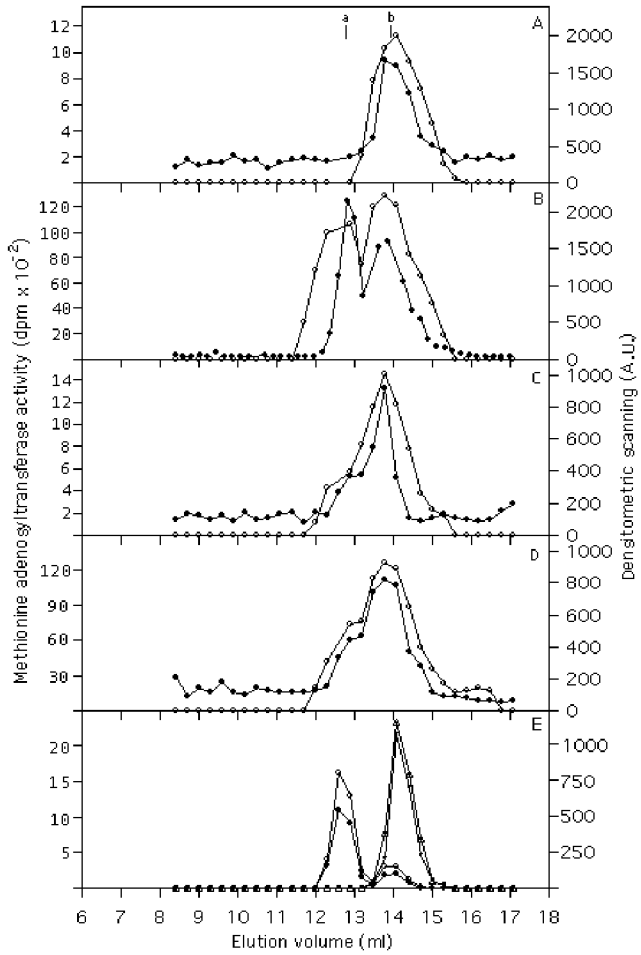

FIG. 1. **Gel filtration chromatography analysis of wild type DTT- and GSH/GSSG-refolded samples.** Wild type MAT was refolded using the DTT or GSH/GSSG refolding methods. Samples of the refolded mixtures (100 μl) were injected on a Superose 12 HR column at two protein concentrations and detected by measuring MAT activity (●) and by densitometric scanning of the dot blots corresponding to each collected fraction (○). *A* and *B* show the profiles for DTT-refolded MAT at 0.2 mg/ml (*A*) and 2 mg/ml (*B*); *C* and *D* depict the profiles for the GSH/GSSG-refolded MAT at 0.2 mg/ml (*C*) and 2 mg/ml (*D*). *E* shows the profile for the rechromatography of MAT I (● and ○) and III (▼ and △) from *D* (the data have been scaled for graphical purposes). Elution positions for rat liver purified MAT I (*point a*) and III (*point b*) are indicated in *A*. The figure shows the results of a typical experiment.

dimers at the protein concentrations used for refolding, but concentration by ultrafiltration caused the apparition of tetramers (Fig. 1, *A* and *B*). On the other hand, replacement of DTT by a GSH/GSSG redox buffer allowed the production of a mixture of tetramers and dimers, which do not associate upon enhancement of the protein concentration (Fig. 1, *C* and *D*). Reloading of both GSH/GSSG-refolded MAT I and III on gel filtration chromatography showed no variation in the elution position for both association states (Fig. 1*E*). These results were confirmed on analytical phenyl Sepharose chromatography, a procedure that allows the quantitative separation of MAT I and III forms by means of differences in hydrophobicity (39). Association was also studied by sedimentation velocity, but the use of this technique was precluded because complete dissociation of tetramers to dimers and monomers was already observed at the highest protein concentrations tested (2 mg/ml).

Dissociation of MAT I was then studied by analytical phenyl Sepharose chromatography. As can be observed, isolated DTT-refolded MAT I render tetramers and dimers upon reloading on

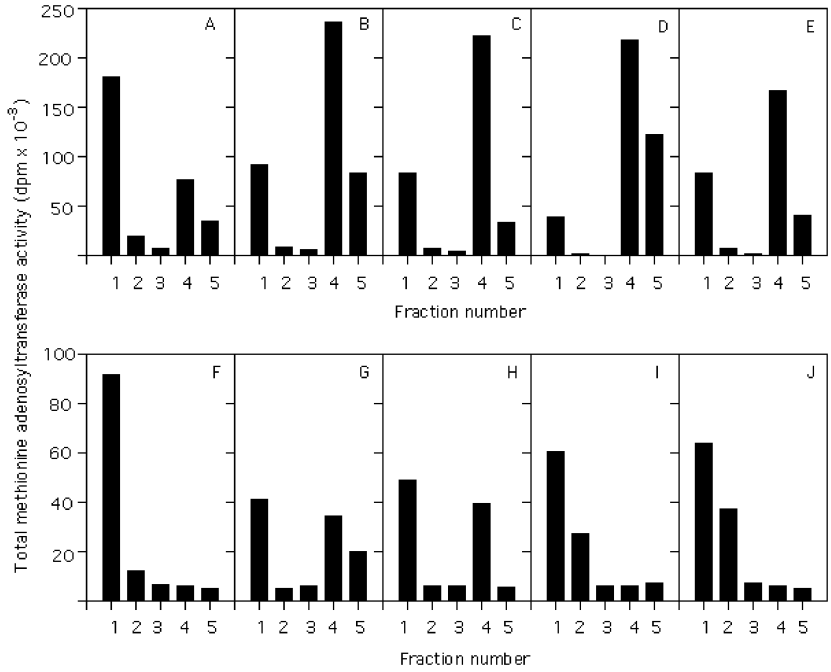

FIG. 2. **Analytical phenyl Sepharose chromatography of DTT- and GSH/GSSH-refolded tetrameric forms of MAT wild type and mutants.** Wild type MAT and cysteine mutants were refolded using the DTT and GSH/GSSG refolding systems and concentrated to 1 mg/ml. Tetramer forms for each sample were separated by phenyl Sepharose chromatography and diluted in the equilibration buffer before reloading on analytical phenyl Sepharose columns. The presence of tetramer and dimer forms was followed by measuring MAT activity. *Fractions 1–3* correspond to sample loading and the washing step, whereas *fractions 4* and *5* are the elution with Me_2SO. *A–E* show the behavior of DTT-refolded tetrameric forms of MAT wild type and mutants, whereas *F–J* depict the results of the GSH/GSSG-refolded tetramers. *A* and *F* correspond to the wild type; *B* and *G* correspond to the C35S mutant; *C* and *H* correspond to the C61S mutant; *D* and *I* correspond to the C57S mutant; and *E* and *J* correspond to the C69S mutant. The figure shows the results of a typical experiment.

the hydrophobic columns, whereas GSH/GSSG-refolded MAT I appears as a stable tetramer (Fig. 2, *A* and *F*). More information about the dissociation process was then obtained by fluorescence spectroscopy of ANS-bound DTT-refolded MAT I samples (Fig. 3*A*). Dilution followed by immediate recording of the fluorescence emission at 470 nm revealed the presence of an exponential decay, until the emission levels corresponding to an ANS-bound dimer were reached (Fig. 3*B*). This decay was preceded by a short lag phase, suggesting the presence of at least one intermediate in the process (Fig. 3*A*, *inset*). The fluorescence intensity of MAT I corresponded to the double of that for MAT III, thus indicating that the dye binds in an area not related to association. This change cannot be followed by intrinsic fluorescence, because no significant changes in the Trp and Tyr emissions were detectable (data not shown). The same is true for other spectroscopic techniques, such as circular dichroism, because MAT I and III show identical spectra. The data were then analyzed using either one- or two-phase exponential decays (Equations 1 and 2), with the best fit being obtained by a single exponential. The calculated rate constant (k_{off}) for dissociation to MAT III is 0.022 s^{-1}, and the calculated half-life for MAT I upon dilution is 14.69 ± 0.5 s at 25 °C. Large-zone gel filtration chromatography was then used for the calculation of the dissociation constants (Fig. 4). Using large zones in the 0.05–5 mg/ml range, the centroid volumes for each protein concentration were calculated and used to determine the weight-average partition coefficients (Equation 3) and the dimer fraction (Equation 4). These data were then used to obtain the K_d value for the DTT-refolded MAT, which was found to be in the 10^5 M^{-1} range (Table I). Moreover, the free energy of association was calculated using this dissociation constant in Equation 6, as well as using the dimer fractions in Equations 5 and 6 (Table I).

Role of the Sulfhydryl Groups in MAT Association—MAT contains 10 cysteine residues/subunit that could be present either in a reduced or partially oxidized pattern. In the present study different oxido/reduction conditions were used for refolding of wild type MAT, and thus several parameters related to the redox status of the protein could differ among the forms obtained. Analysis of the free −SH group content of the different MAT forms was carried out by NEM or vinylpyridine labeling followed by mass spectrometry (Table II). The molecular mass of DTT-refolded MAT was 43,518 Da, which changed to 44,549 Da after treatment with vinylpyridine under denaturing but nonreducing conditions (Fig. 5, *A* and *B*). This value was not altered by reduction of the protein followed by ethylpyridilation. The mass difference of 1031 Da corresponded to the addition of 10 (1031/106 = 9.7) EP groups, thus indicating that the 10 −SH groups of the DTT-refolded MAT subunit were accessible. On the other hand, the molecular mass of the GSH/GSSG-refolded MAT I and III increased by 823 Da upon treatment with vinylpyridine under denaturing but nonreducing conditions, and by 1061 Da when the proteins were fully reduced and ethylpyridilated (Fig. 5*C*). These results showed that the GSH/GSSG-refolded proteins contained eight titrable cysteine residues and a disulfide bond.

The redox behavior of these proteins was further characterized. Wild type MAT refolded using both procedures is inhibited by GSSG, but the K_i values calculated are lower for the GSH/GSSG-refolded forms, indicating a higher susceptibility to this agent (Table II). In addition, modulation of the activity by redox buffers is also observed, and the K_{ox} values were calculated on the basis of the previous knowledge for this enzyme (Table III). These values are close to the R[GSH] data determined *in vivo* under mild to severe oxidative stress (300–3 mM) (40).

C35S and C61S Mutations Abrogate the Oligomer Interconversion Blockage—The results presented above prompted us to explore the possibility that the presence of a disulfide bond could be responsible for the differences observed among DTT- and GSH/GSSG-refolded MATs. For this purpose, individual mutants on cysteine residues located at the dimer-dimer contact area, according to the crystal structure of the protein, were selected. Of the 10 cysteine residues of the MAT polypeptide chain, four are located at the β-sheet (B2) of contact between dimers (Cys^{35}, Cys^{57}, Cys^{61}, and Cys^{69}) (Fig. 6). Among those, Cys^{61} and Cys^{69} are specific for the liver enzyme and hence may be directly linked to the special behavior shown by this MAT. These four residues were mutated to serine, and the recombinant proteins were refolded using either the DTT or GSH/GSSG system described above and purified. Characterization by CD and fluorescence spectroscopy showed no differ-

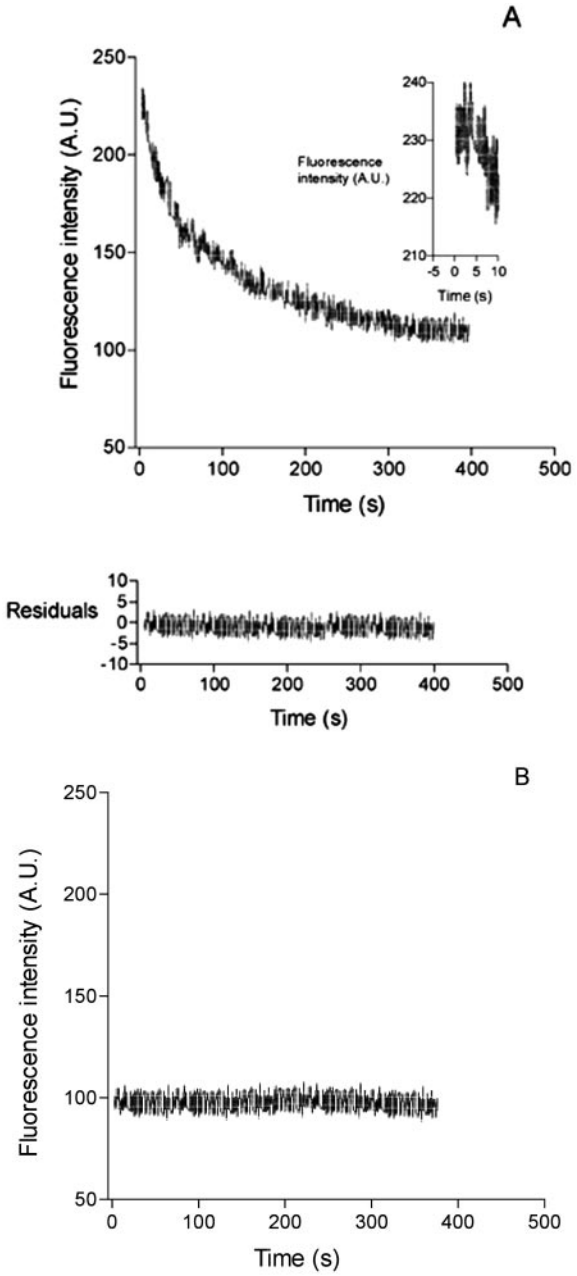

FIG. 3. **Kinetics of MAT I dissociation followed by ANS fluorescence.** Wild type MAT was DTT-refolded and purified. A concentrated sample (4 mg/ml), MAT I, was incubated with ANS and diluted to 0.08 mg/ml immediately before recording fluorescence at 470 nm (*A*). The *inset* shows an enlargement of the initial phases of the reaction. Samples of MAT III (0.08 mg/ml) were also incubated with ANS, and their fluorescence was recorded (*B*). The data were fitted to one- or two-phase exponential decays as described under "Experimental Procedures."

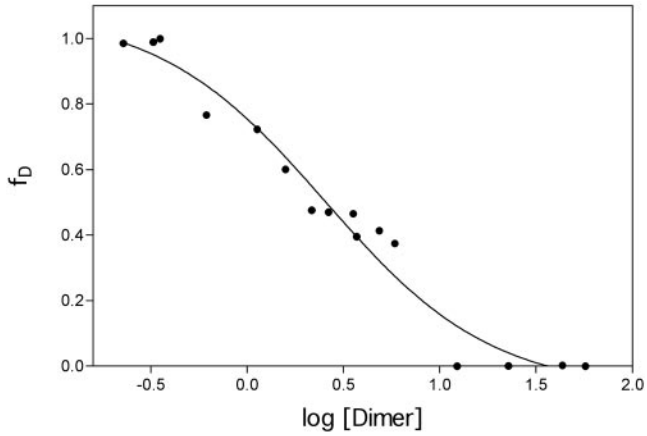

FIG. 4. **Determination of the K_d for wild type MAT by large-zone gel filtration chromatography.** Large zones for several protein concentrations (0.05–5 mg/ml) were loaded on a gel filtration column. A_{280} was recorded, and fractions of the eluent were collected for its use in dot blot. The centroid volume for each zone was determined and used for the calculation of the weight-average partition coefficient and the f_D. The K_d value was calculated from the plot of f_D *versus* log of the dimer concentration (μM). The figure shows a plot of a typical experiment for DTT-refolded wild type MAT.

TABLE I

Dissociation constants and free energies of the association process

The K_d values were calculated using the fraction of dimer deduced from the centroid volume of the large-zone gel filtration chromatography, using a protein concentration range from 0.05 to 5 mg/ml. $\Delta G(H_2O)$ was calculated by two methods. $\Delta G(H_2O)^1$ was obtained using K_d values in Equation 6, whereas $\Delta G(H_2O)^2$ was calculated from the same dimer fractions using equations analogous to those of Park and Bedouelle for a monomer-dimer equilibrium.

	K_d	$\Delta G(H_2O)^1$	$\Delta G(H_2O)^2$
	M^{-1}	*kcal/mol*	*kcal/mol*
DTT refolding			
Wild type	$(3.66 \pm 0.64)\ 10^5$	-7.58 ± 1.3	-6.99 ± 0.1
C35S	$(10.79 \pm 0.68)\ 10^5$	-8.22 ± 0.54	-7.79 ± 0.88
C61S	$(14.83 \pm 0.78)\ 10^5$	-8.41 ± 0.45	-9.34 ± 0.14
GSH/GSSG refolding			
Wild type	—[a]	—	—
C35S	$(10.01 \pm 0.47)\ 10^5$	-8.18 ± 0.39	-8.71 ± 0.97
C61S	$(7.54 \pm 0.29)\ 10^5$	-8.01 ± 0.3	-7.92 ± 0.74

[a] —, not determined because of the absence of MAT I/III equilibrium.

ence as compared with the wild type protein. However, whereas the specific activity recovered upon refolding paralleled that for each mutant in the cytosolic fraction, purification of the refolded proteins led to changes in the enzymatic behavior; those related to C69S are especially important. This mutant shows low activity (20% of the wild type) in the cytosolic fraction and appears mainly as dimers, whereas once DTT-refolded and purified its specific activity increases to about 64% (70 nmol/min/mg) of that shown by the wild type, MAT and tetramers can be detected. Moreover, all of the refolded mutants have sigmoidal kinetics, but the affinity shown by C61S for both substrates was reduced (Table III).

The capacity of association of the DTT- and GSH/GSSG-refolded mutants was then explored. As can be observed, all of them are in tetramer-dimer equilibrium upon DTT refolding, a behavior that is conserved in C35S and C61S after GSH/GSSG refolding (Fig. 2). The molecular masses of these MAT mutants, determined after vinylpyridine labeling by MALDI-TOF mass spectrometry were 44,455 Da (Fig. 5*D*), indicating the presence of nine free −SH groups in C35S and C61S under both refolding conditions (Table III). Dissociation constants were also calculated by large-zone gel filtration chromatography, the values being larger than that for the wild type MAT (Table I). On the other hand, stable MAT I/III forms were obtained when using the redox buffer system to refold C57S and C69S (Fig. 2). The fact that the association process is still observed in the absence of Cys^{35} and Cys^{61} is consistent with a role for these residues in the oligomerization process.

Identification of the Disulfide Bond in GSH/GSSG-refolded MAT—To ensure that a disulfide bridge between Cys^{35} and Cys^{61}, such as that detected in liver-purified MAT, is responsible for the blockage of association, free sulfhydryls of GSH/GSSG-refolded wild type MAT were ethylpyridylated (EP) or carboxyamidomethylated (CM), and the native and the EP- and CM-GSH/GSSG-refolded wild type MAT proteins were degraded with CNBr and trypsin. The proteins and their diges-

TABLE II
Molecular and enzymatic features of wild-type refolded-MAT I/III

Wild type MAT samples were refolded with DTT or GSH/GSSG, and the oligomeric forms obtained were characterized and analyzed for their −SH content and their behavior against GSSG and GSH/GSSG buffers. The data on the table are the means ± S.D. of the results obtained in experiments carried out in triplicate for the refolded MAT I/III.

	DTT-refolded MAT III	GSH/GSSG-refolded MAT III	GSH/GSSG-refolded MAT I
M_r on gel filtration chromatography	92,700	89,125	194,900
Specific activity (nmol/min/mg)	110 ± 11	95.8 ± 4.4	100.3 ± 13.1
Free −SH groups	10.35 ± 0.4	8.04 ± 0.4	8.02 ± 0.3
K_i GSSG (mM)	2.15 ± 0.48	0.42 ± 0.07	1.02 ± 0.41
$R_{0.5}$ GSH/GSSG	4.01 ± 1.32	3.88 ± 0.41	6.27 ± 0.96
K_{ox} (mM)	40.1	38.8	62.7

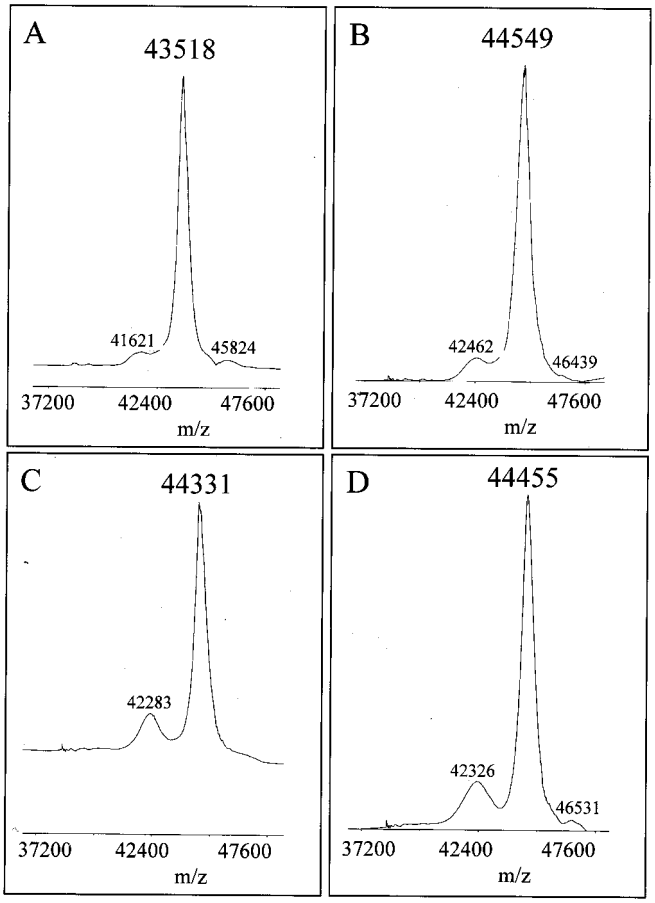

FIG. 5. **MALDI-TOF mass spectrometry.** Mass spectrometric determination of the molecular masses of DTT-refolded MAT before (*A*) and after (*B*) treatment with vinylpyridine under denaturing but nonreducing conditions is shown. Molecular masses of GSH/GSSG-refolded MAT I and III (*C*) and of C35S and C61S MAT mutants (*D*) upon treatment with vinylpyridine under denaturing but nonreducing conditions are also included.

tion products were analyzed by MALDI-TOF mass spectrometry. The isotope-averaged (±8 Da) molecular masses of native and EP-GSH/GSSG-refolded wild type MATs were 43,507 and 44,328 Da, respectively (Table IV). The mass difference of 824 Da indicated the presence of 7.8 titrable sulfhydryl groups. On the other hand, both reduced and EP-GSH/GSSG-refolded wild type MAT proteins showed the same molecular mass of 44,565 Da (Table IV). Thus, fully reduced MAT proteins contained 10 EP-cysteine residues. As a whole, these results indicated the presence of one disulfide bond and eight sulfhydryl groups in GSH/GSSG-refolded wild type MAT. CNBr degradation of GSH/GSSG-refolded MAT yielded a fragment of 5816 Da, which corresponded to the stretch 21–75 with Met^{65} as sulfoxide. This polypeptide contains four cysteine residues, those at positions 35, 57, 61, and 69. On the other hand, the fragment 21–77 with Met^{65} sulfoxide and two EP-cysteines ($M + H^+$ 6230) was characterized upon CNBr degradation of EP-GSH/GSSG-refolded MAT. Hence, GSH/GSSG-refolded MAT contained two free cysteines and a disulfide bond within the stretch comprising residues 21–75. When carboxyamidomethylated GSH/GSSG-refolded MAT was digested with trypsin and analyzed by mass fingerprinting MALDI-TOF mass spectrometry, tryptic fragments containing CM-cysteine residues 69, 105, 121, 150, 312, and 377 were found (Table IV). On the other hand, the ion of m/z = 6588.3 corresponded to the polypeptide stretch 2–62 with two CM-cysteines, one disulfide bond, and Met^{20} oxidized. These results indicate the existence of a disulfide bond involving two cysteines among 9, 35, 57, and 61. Furthermore, the ion of m/z = 2551.9 was assigned to fragments 34–48 disulfide bonded to 55–62, containing a CM-cysteine and a disulfide bond. This allowed the identification of Cys^{35} as one of the residues forming part of the disulfide with either Cys^{57} or Cys^{61}. These results, together with the fact that Cys^{61}, but not Cys^{57}, is at S–S bonding distance from Cys^{35} in the crystal structure (Protein Data Bank accession code 1QM4) (Fig. 6), strongly support the possibility that Cys^{35} and Cys^{61} are disulfide-bonded in GSH/GSSG-refolded MAT.

DISCUSSION

MAT isoforms, as purified from the liver, appear as stable dimers and tetramers, whereas the recombinant protein, as isolated from *E. coli*, shows a concentration-dependent equilibrium between MAT I and III (29). These behaviors are paralleled by the MAT forms generated under two different refolding systems, DTT- and GSH/GSSG-based (31), thus providing a useful tool to explore the mechanisms that control association. Analysis of the association process by analytical ultracentrifugation techniques evidenced a dramatic sensitivity of the oligomeric assemblies to centrifugal forces. This phenomenon, experimentally manifested as dissociation, has been described in other oligomeric proteins, such as NAD-dependent dehydrogenases and tryptophan synthase (41). This instability can be explained by the low number of interactions between dimers shown in the MAT I crystal structure (28) (Fig. 7). In fact, only five polar interactions have been described to take place between dimers in contrast to what happens in the *E. coli* MAT (c-MAT) (42). In this last case the number of interactions between dimers in the tetramer structure is far larger than in MAT I, and no dimer structures have been obtained to date. Moreover, the particular arrangement of interactions observed is completely different to that shown in the crystal structure of c-MAT (Fig. 7). Rat liver presents a squared contact area formed by residues of its four subunits that is in direct contact with the solvent. On the other hand, c-MAT has this squared area surrounded by a larger contact area that precludes its exposure to the solvent, thus protecting those interactions and allowing a higher stability for the complex. Based on these considerations the techniques of choice for our experi-

TABLE III
Characterization of the refolded MAT III forms

Wild type MAT and mutants C35S and C61S were refolded in the presence of either DTT- or GSH/GSSG-containing buffers. The dimeric forms were purified in each case and characterized kinetically. In addition, samples were used for free −SH determination by MALDI-TOF. The data shown are the means ± S.D. of three independent experiments carried out in triplicate.

	V_{max}	$S_{0.5}$ Met	$S_{0.5}$ ATP	Free −SH groups
	nmol/min/mg	*μM*	*μM*	
DTT-refolded				
Wild type	110 ± 11	246 ± 76	588 ± 108	9.7
C35S	94.47 ± 6.3	222 ± 61	493 ± 47.5	8.9
C61S	69.07 ± 16.5	756 ± 31.9	3250 ± 220	9.3
GSH/GSSG-refolded				
Wild type	95.8 ± 4.4	1120 ± 150	530 ± 48	7.8
C35S	32.7 ± 0.56	449.6 ± 17.7	777.6 ± 47.8	9.1
C61S	31.5 ± 0.21	793.8 ± 129.2	2540 ± 130	8.7

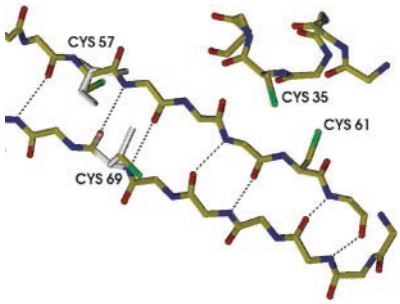

FIG. 6. **Localization of Cys^{35}, Cys^{57}, Cys^{61}, and Cys^{69} in rat liver MAT I crystal structure.** The figure shows the two strands of β-sheet B2, where Cys^{57}, Cys^{61}, and Cys^{69} are located (Protein Data Bank code 1QM4). In addition, the position of Cys^{35} on α-helix 1 is also included. Sulfhydryl groups are shown in *green*, and the *dashed lines* indicate the hydrogen bonds stabilizing the β-sheet. In *gray* are the positions that Cys^{57} and Cys^{69} should have to form a disulfide bond.

ments were gel filtration and analytical phenyl Sepharose chromatographies.

Hydrophobic chromatography was described by Kunz *et al.* (39) as a way to separate MAT I and III, because of the high avidity shown by MAT III for phenyl Sepharose, and has been used as a quantitative method to establish the ratio of isoforms (29). Therefore, association and dissociation of the refolded MATs were followed by this method, whereas calculation of the dissociation constants was performed using large-zone gel filtration chromatography as described by Beckett (33). The K_d values obtained either for wild type and mutants were in the 10^5 M^{-1} range, a value comprised between those described for proteins showing association/dissociation behavior (43). These values are in agreement with those previously obtained for the cytosolically overexpressed wild type MAT (29) and much lower than that for c-MAT, which was calculated to be 10^{10} M^{-1} (44). In addition, K_d values were also used to calculate the free energy of association to MAT I, and the values in all of the cases were of the same order, −7 to −8 kcal/mol, again similar to the values obtained for proteins showing association processes (33, 45). These refolded forms present a higher susceptibility to inhibition by GSSG as compared with the liver purified-MAT, but their oxidation constants are in the range for a regulation under mild to severe oxidative stress (40). On the other hand, the calculated half-life for the tetramer is shorter than that previously published for the cytosolically overexpressed MAT (14.69 *versus* 858 s), where the temperature is the main difference between both experiments (29).

Differences among the refolding systems used are based in their redox potential; thus it could be possible that the opposite association behavior shown by DTT- and GSH/GSSG-refolded MAT may be due to an effect related to the redox state of the cysteine sulfhydryls. MAT polypeptide contains

TABLE IV
Results of the tryptic digestion analyzed by MALDI-TOF mass spectrometry

Fragments assigned by MALDI-TOF mass spectrometry in GSH/GSSG-refolded MAT III digested with trypsin under denaturing but nonreducing conditions in the presence of 10 mM iodoacetamide.

M + H$^+$	Fragment	Sequence modifications
Da		
2551.9	34–48	
	55–62	1 CM-C; 1 S-S
6588.3	2–62	2 CM-C; 1 S-S; M20-ox
672.7	49–54	
2308.6	63–82	CM-C69; 1 M-ox
2264.8	63–82	C69-red; 2 M-ox
2233.1	63–82	C69-red
1006.0	80–98	
3261.1	99–126	CM-C105; CM-C121
2553.9	104–126	C105 and C121 red
3775.2	127–160	CM-C150; M139-ox; M151-ox
503.6	161–164	
605.1	165–169	
4969.5	127–170	CM-C150
1510.2	170–182	
1354.8	171–182	
3321.8	171–200	
1988.2	183–200	
2306.3	201–220	
1622.8	221–235	
1182.6	225–235	
584.7	230–235	
1806.9	236–250	
1430.8	251–265	
1080.4	291–300	
1621.9	294–308	
446.2	305–308	
576.7	309–313	CM-C312
942.5	345–352	
1286.5	353–363	
1025.2	355–363	
603.7	364–368	
1069.1	375–383	CM-C377
1118.6	384–392	

10 such residues/subunit that under the redox buffer could originate reduced or partially oxidized proteins (19, 20). Our results indicate that two of the 10 −SH groups are not accessible to alkylation, even after guanidinium chloride denaturation, thus suggesting their involvement in a disulfide. These residues have been identified using single cysteine mutants as Cys^{35} and Cys^{61}, the same residues involved in the disulfide bond identified in rat liver-purified MAT isoforms (15). The conclusions from these studies with mutant proteins are in line with mass spectrometry analysis of CNBr and trypsin degradation products of EP- or CM-GSH/GSSG-refolded MAT. Moreover, GSH/GSSG refolding of these mutants preserves the concentration-dependent equilibrium, clearly indicating the importance of Cys^{35} and Cys^{61} in the

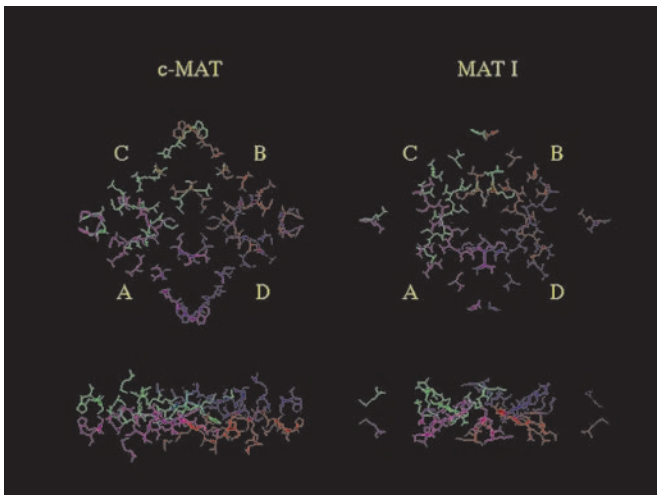

FIG. 7. **Dimer-dimer contact areas in c-MAT and rat liver MAT I.** The figure shows two views of the dimer-dimer contact areas for *E. coli* (Protein Data Bank code 1FUG) and rat liver MATs (Protein Data Bank code 1QM4), the only two proteins of this family whose crystal structure has been determined. Subunits are shown under different colors: *magenta* (*A*), *red* (*B*), *green* (*C*), and *blue* (*D*).

association. The presence of these cysteines in the β-sheet of contact between dimers and the fact that Cys^{61} is a liver-specific amino acid may be related to the special features shown by the liver-specific MAT, such as its capacity to generate two oligomeric assemblies (16). In fact, the sulfhydryls of these two cysteines appear perfectly oriented and at bonding distance in the crystal structure of MAT I (obtained in the presence of DTT) (28). As for Cys^{57} and Cys^{69} (another liver-specific cysteine), both are also located in the β-sheet B2 and close enough as to form a disulfide bond, but their sulfhydryl groups are facing opposite directions (Fig. 6). Thus, it could be possible that under certain circumstances this second disulfide is formed, but for this purpose a slight torsion of the main chain of the protein would be needed. Therefore, it can be deduced that alterations in this β-sheet of contact could be responsible for the changes observed in the oligomerization.

Intramolecular disulfides are known to have a role in protein oligomerization (46) but are not commonly observed in such a reducing environment as cellular cytosol (10, 14). However, during folding it is possible that a large increase in the local sulfhydryl concentration occurs, allowing the production of disulfides. Moreover, *in vitro* experiments have shown the production of optimal oxidation rates during folding, even in the presence of significant concentrations of reductants (13). *In vivo*, using alcohol liver cirrhotic samples, an increase in the oxidation conditions is also observed that was caused by a 30% reduction in the GSH levels. Under these conditions a decrease in MAT activity correlated with its apparition mainly as dimers has been described (27), but no explanation for this incapacity to associate has been obtained for the moment. Based on our data, we suggest that under cirrhotic oxidative conditions the production of dimers may be favored by allowing the disulfide bond (Cys^{35}–Cys^{61}) to form, before association to MAT I takes place. Another possibility that cannot yet be excluded is the production of another disulfide (Cys^{57}–Cys^{69}) or of both disulfide bridges (Cys^{35}–Cys^{61} and Cys^{57}–Cys^{69}) in cirrhotic MAT dimers. In these cases, association may not be precluded exclusively by the presence of the disulfide bonds but also by the incapacity of establishing the correct polar interactions on the interface, because of the main chain torsion. Moreover, a third possibility exists: the presence of two types of dimers. Our results on the kinetics of MAT I dissociation suggest the presence of an intermediate in the pathway to MAT III. Even when it is not possible to infer the oligomeric state of such an intermediate, it is attractive to suggest that it may be a dimer just separated from MAT I, before undergoing the small changes that lead to MAT III. These changes should occur close to the ANS-binding site, located between Pro^{358}-Gly^{359} and the sequence Val-Gly-Ala that limits the active-site loop as suggested by Sánchez del Pino *et al.* (47), because a kinetic intermediate is detectable by this modification. All of these data together showing the effects exerted by dissociation on areas related to the active site, such as the flexible loop and the central domain may explain the 10-fold decrease in methionine affinity shown by MAT III as compared with MAT I or its activation by Me_2SO (2, 17).

Using the previous knowledge on MAT III urea unfolding (47, 48) and the results described herein, we propose the following model for MAT I folding and association.

$$\text{MAT I} \leftrightarrow 2I_k^1 \leftrightarrow 2\ \text{MAT III} \leftrightarrow 4I_k^2 \leftrightarrow 4I \leftrightarrow 4U$$

MODEL 1

The unfolded MAT polypeptide (*U*) associates to the dimer (MAT III) through a monomeric equilibrium-intermediate (*I*), which evolves to a monomeric kinetic intermediate (I_k^2). The dimer (MAT III) could then undergo oxidation of Cys^{35} and Cys^{61} to make a disulfide bond that precludes further association or evolve to a kinetic intermediate (I_k^1) that leads to the tetramer (MAT I). The production of the Cys^{35}–Cys^{61} disulfide in MAT I must then take place in this last kinetic intermediate before definitive association in the tetramer. The total free energy of the process can be calculated using Equation 7, and in our case this renders a $\Delta G(H_2O)$ of 24.41 kcal/mol.

Finally, all of these results indicate that the presence of a disulfide bond between Cys^{35} and Cys^{61} is responsible for the stabilization of tetramer and dimer forms, blocking the association process. The production of this disulfide takes place at the dimer level (MAT III and I_k^1).

Acknowledgments—We thank Francisco Garrido for technical assistance, Dr. J. L. Neira for the critical comments of the manuscript, and Dr. D. Laurents and B. Ashley Morris for grammatical and English style corrections.

REFERENCES

1. Cappel, R. E., and Gilbert, H. F. (1988) *J. Biol. Chem.* **263,** 12204–12212
2. Pajares, M. A., Durán, C., Corrales, F., Pliego, M. M., and Mato, J. M. (1992) *J. Biol. Chem.* **267,** 17598–17605
3. Ferreras, M., Gavilanes, J. G., Lopez-Otín, C., and Garcia-Segura, J. M. (1995) *J. Biol. Chem.* **270,** 28570–28578
4. Zhang, F. L., and Casey, P. J. (1996) *Annu. Rev. Biochem.* **65,** 241–269
5. Nalivaeva, N. N., and Turner, A. J. (2001) *Proteomics* **1,** 735–747
6. Stamler, J. S., Lamas, S., and Fang, F. C. (2001) *Cell* **106,** 675–683
7. Laity, J. H., Lee, B. M., and Wright, P. E. (2001) *Curr. Opin. Struct. Biol.* **11,** 39–46
8. Creighton, T. E. (1984) *Methods Enzymol.* **107,** 305–329
9. Creighton, T. E. (1986) *Methods Enzymol.* **131,** 83–106
10. Silva, C. M., and Cidlowsky, J. A. (1989) *J. Biol. Chem.* **264,** 6638–6647
11. Hardy, S. J., Holmgren, J., Johansson, S., Sánchez, J., and Hirst, T. R. (1988) *Proc. Natl. Acad. Sci. U. S. A.* **85,** 7109–7113
12. Price, N. C. (1994) *Mechanisms of Protein Folding* (Pain, R. H., ed) pp. 160–193, IRL Press, Oxford, UK
13. Gilbert, H. F. (1994) *Mechanisms of Protein Folding* (Pain, R. H., ed) pp. 104–136, IRL Press, Oxford, UK
14. Davoodi, J., Drown, P. M., Bledsoe, R. K., Wallin, R., Reinhart, G. D., and Hutson, S. M. (1998) *J. Biol. Chem.* **273,** 4982–4989
15. Martínez-Chantar, M. L., and Pajares, M. A. (2000) *Eur. J. Biochem.* **267,** 132–137
16. Mato, J. M., Alvarez, L., Ortiz, P., and Pajares, M. A. (1997) *Pharmacol. Ther.* **73,** 265–280
17. Cabrero, C., Puerta, J. L., and Alemany, S. (1987) *Eur. J. Biochem.* **170,** 299–304
18. Cantoni, G. L. (1975) *Annu. Rev. Biochem.* **44,** 435–451
19. Horikawa, S., Ishikawa, M., Ozasa, H., and Tsukada, K. (1989) *Eur. J. Biochem.* **184,** 497–501
20. Alvarez, L., Asunción, M., Corrales, F., Pajares, M. A., and Mato, J. M. (1991) *FEBS Lett.* **290,** 142–146
21. Corrales, F., Cabrero, C., Pajares, M. A., Ortiz, P., Martín-Duce, A., and Mato,

J. M. (1990) *Hepatology* **11,** 216–222
22. Pajares, M. A., Corrales, F. J., Ochoa, P., and Mato, J. M. (1991) *Biochem. J.* **274,** 225–229
23. Mingorance, J., Alvarez, L., Sánchez-Góngora, E., Mato, J. M., and Pajares, M. A. (1996) *Biochem. J.* **315,** 761–766
24. Avila, M. A., Mingorance, J., Martínez-Chantar, M. L., Casado, M., Martín-Sanz, P., Boscá, L., and Mato, J. M. (1997) *Hepatology* **25,** 391–396
25. Sánchez-Góngora, E., Ruiz, F., Mingorance, J., An, W., Corrales, F. J., and Mato, J. M. (1997) *FASEB J.* **11,** 1013–1019
26. Corrales, F., Ochoa, P., Rivas, C., Martín-Lomas, M., Mato, J. M., and Pajares, M. A. (1991) *Hepatology* **14,** 528–533
27. Cabrero, C., Martín-Duce, A., Ortiz, P., Alemany, S., and Mato, J. M. (1988) *Hepatology* **8,** 1530–1534
28. González, B., Pajares, M. A., Hermoso, J., Alvarez, L., Garrido, F., Sufrin, J. R., and Sanz-Aparicio, J. (2000) *J. Mol. Biol.* **300,** 363–375
29. Mingorance, J., Alvarez, L., Pajares, M. A., and Mato, J. M. (1997) *Int. J. Biochem. Cell Biol.* **29,** 485–491
30. Alvarez, L., Mingorance, J., Pajares, M. A., and Mato, J. M. (1994) *Biochem. J.* **301,** 557–561
31. López-Vara, M. C., Gasset, M., and Pajares, M. A. (2000) *Protein Expression Purif.* **19**, 219–226
32. Haugland, R. P. (1991) *Handbook of Fluorescent Probes and Research Chemicals*, Molecular Probes, Inc., Eugene, OR
33. Beckett, D. (1999) *Current Protocols in Protein Science* (Coligan, J. E., Dunn, B. M., Speicher, D. W., and Wingfield, P. T., eds) pp. 20.5.1–20.5.13, John Wiley & Sons Inc., New York
34. Park, Y. C., and Bedouelle, H. (1998) *J. Biol. Chem.* **273,** 18052–18059
35. Philo, J. S. (1997) *Biophys. J.* **72,** 435–444
36. van Holde, K. E. (1986) *Physical Biochemistry*, 2nd Ed., pp. 110–136, Prentice-Hall, Uppersaddle River, NJ
37. Gil, B., Pajares, M. A., Mato, J. M., and Alvarez, L. (1997) *Endocrinology* **138,** 1251–1258
38. Martínez-Chantar, M. L., and Pajares, M. A. (1996) *FEBS Lett.* **397,** 293–297
39. Kunz, G. L., Hoffman, J. L., Chia, C., and Stremel, B. (1980) *Arch. Biochem. Biophys.* **202,** 565–572
40. Gilbert, H. K. (1989) *Glutathione Centennial: Molecular Perspectives and Clinical Implications* (Taniguchi, T., Higashi, T., Sakamoto, Y., and Meister, A., eds) pp. 73–87, Academic Press, New York
41. Gross, M., and Jaenicke, R. (1994) *Eur. J. Biochem.* **221,** 617–630
42. Takusagawa, F., Kamitori, S., Misaki, S., and Markham, G. D. (1996) *J. Biol. Chem.* **271,** 136–147
43. Friedman, F. K., and Beychok, S. (1979) *Annu. Rev. Biochem.* **48,** 217–250
44. Markham, G. D., and Satishchandran, C. (1988) *J. Biol. Chem.* **263,** 8666–8670
45. Ip, S. H. C., and Ackers, G. K. (1977) *J. Biol. Chem.* **252,** 82–87
46. Marchand, P., Volkmann, M., and Bond, J. S. (1996) *J. Biol. Chem.* **271,** 24236–24241
47. Sánchez del Pino, M. M., Pérez-Mato, I., Sanz, J. M., Mato, J. M., and Corrales, F. J. (2002) *J. Biol. Chem.* **277,** 12061–12066
48. Gasset, M., Alfonso, C., Neira, J. L., Rivas, G, and Pajares, M. A. (2002) *Biochem. J.* **361,** 307–315

Role of an Intrasubunit Disulfide in the Association State of the Cytosolic Homo-oligomer Methionine Adenosyltransferase

Gabino F. Sánchez-Pérez, Mari?a Gasset, Juan J. Calvete and Mari?a A. Pajares

J. Biol. Chem. 2003, 278:7285-7293.
doi: 10.1074/jbc.M210177200 originally published online December 20, 2002
